Journal of Biomedical Optics

BiomedicalOptics.SPIEDigitalLibrary.org

Optical metabolic imaging of irradiated rat heart exposed to ischemia–reperfusion injury

Mette Funding la Cour
Shima Mehrvar
James S. Heisner
Mohammad Masoudi Motlagh
Meetha Medhora
Mahsa Ranji
Amadou K. S. Camara

Mette Funding la Cour, Shima Mehrvar, James S. Heisner, Mohammad Masoudi Motlagh, Meetha Medhora, Mahsa Ranji, Amadou K. S. Camara, "Optical metabolic imaging of irradiated rat heart exposed to ischemia–reperfusion injury," *J. Biomed. Opt.* **23**(1), 016011 (2018), doi: 10.1117/1.JBO.23.1.016011.

SPIE.

Optical metabolic imaging of irradiated rat heart exposed to ischemia–reperfusion injury

Mette Funding la Cour,[a,†] Shima Mehrvar,[a,†] James S. Heisner,[b] Mohammad Masoudi Motlagh,[a] Meetha Medhora,[c] Mahsa Ranji,[a,*,‡] and Amadou K. S. Camara[b,*,‡]
[a]University of Wisconsin Milwaukee, Department of Electrical Engineering, Milwaukee, Wisconsin, United States
[b]Medical College of Wisconsin, Department of Anesthesiology and Cardiovascular Research Center, Milwaukee, Wisconsin, United States
[c]Medical College of Wisconsin, Department of Radiation Oncology, Milwaukee, Wisconsin, United States

Abstract. Whole thoracic irradiation (WTI) is known to cause deterioration in cardiac function. Whether irradiation predisposes the heart to further ischemia and reperfusion (IR) injury is not well known. The aim of this study is to examine the susceptibility of rat hearts to IR injury following a single fraction of 15 Gy WTI and to investigate the role of mitochondrial metabolism in the differential susceptibility to IR injury. After day 35 of irradiation, *ex vivo* hearts from irradiated and nonirradiated rats (controls) were exposed to 25-min global ischemia followed by 60-min IR, or hearts were perfused without IR for the same protocol duration [time controls (TC)]. Online fluorometry of metabolic indices [redox state: reduced nicotinamide adenine dinucleotide (NADH), oxidized flavin adenine dinucleotide (FAD), and NADH/FAD redox ratio] and functional variables [systolic left ventricular pressure (LVP), diastolic LVP (diaLVP), coronary flow (CF), and heart rate were recorded in the beating heart; developed LVP (dLVP) and rate pressure product (RPP)] were derived. At the end of each experimental protocol, hearts were immediately snap frozen in liquid N_2 for later three-dimensional imaging of the mitochondrial redox state using optical cryoimaging. Irradiation caused a delay in recovery of dLVP and RPP after IR when compared to nonirradiated hearts but recovered to the same level at the end of reperfusion. CF in the irradiated hearts recovered better than the control hearts after IR injury. Both fluorometry and 3-D cryoimaging showed that in WTI and control hearts, the redox ratio increased during ischemia (reduced) and decreased on reperfusion (oxidized) when compared to their respective TCs; however, there was no significant difference in the redox state between WTI and controls. In conclusion, our results show that although irradiation of rat hearts compromised baseline cardiovascular function, it did not alter cardiac mitochondrial redox state and induce greater susceptibility of these hearts to IR injury. [DOI: 10.1117/1.JBO.23.1.016011]

Keywords: optical cryoimaging; mitochondria; ischemia and reperfusion; irradiation; redox state.

Paper 170581R received Aug. 31, 2017; accepted for publication Dec. 12, 2017; published online Jan. 19, 2018.

1 Introduction

The two main causes of death in the United States are heart disease and cancer.[1] Studies have shown that the two may be interconnected in radiotherapy during treatment of intrathoracic malignancies.[2] Indeed, radiation is an independent risk factor for death from cardiovascular disease in cancer patients after prolonged thoracic radiotherapy.[2] Exposure to radiation is not limited to radiotherapy.[3–6] Survivors of atomic bombs,[7,8] nuclear accidents, radiologic terrorism, space travel, and radiology imaging[9] are other examples of radiation that could have detrimental cardiovascular effects. After the 9/11 terrorist act, the United States government initiated a program to define and mitigate potential injuries to different organs by a nuclear attack. Overall, this paper explores the potential susceptibility of the ischemic heart to further injury after exposure to ionizing radiation.

Insofar as cardiomyocytes are well-differentiated and nonproliferating cells, the heart is perceived as relatively radiation-resistant as compared to other tissues, such as bone marrow, gut, or lungs.[10,11] Therefore, it has been suggested that radiation damage to the heart is primarily caused by inflammatory changes in the microvasculature with reduced number of capillaries, leading to occlusion of vessels, reduced vascular density, perfusion defects and eventually myocardial ischemia, cell death, and fibrosis.[2,12–15] Two phases of radiation injuries to the whole body have been reported: acute radiation syndrome in which symptoms occur immediately to a few weeks after exposure and delayed effects in which symptoms develop after months to years.[16,17] Thus, the manifestation of cardiovascular disease is more likely to occur with higher dose and longer time exposure to irradiation; hence, the potential for short-term low-dose irradiation-induced injuries is less likely to occur in the heart. Evidence indicates that there are compelling associations between high therapeutic doses of thoracic radiation and increased risks for cardiovascular disease in long-term cancer survivors.[3–6] The incidence of stroke and cardiac ischemic attack is greater with radiation exposed patients compared to the general population.[2] Single-dose irradiation of 20 to 40 Gy in experimental animals has also been associated with cardiac dysfunction due to inflammatory responses.[14]

Thus, for both short- and long-term irradiation exposures, there have been studies of various parameters for examining the impact of radiation on cardiac function in different animal models,[10,16–21] but how a single dose whole thoracic irradiation (WTI) impacts mitochondrial metabolism and ability of

*Address all correspondence to: Mahsa Ranji, E-mail: ranji@uwm.edu; Amadou K. S. Camara, E-mail: aksc@mcw.edu

†Both contributed equally and are therefore first authors.

‡Cosenior authors.

1083-3668/2018/$25.00 © 2018 SPIE

irradiated hearts to withstand ischemia and reperfusion injury (IR) has not been well studied. In the present study, we investigated the impact of a single low dose 15 Gy WTI on cardiac and mitochondrial function before, during, and after global *ex vivo* IR injury. Our aims were: (a) to determine whether WTI predisposes the myocardium to worsened outcome following IR injury and (b) whether altered mitochondria metabolism, specifically redox state, is a key contributor to WTI aggravated IR injury.

IR causes injury to the myocardium, and these injuries are commonly encountered in clinical settings, such as heart transplant, acute myocardial infarction, or crush injury to the chest.[22,23] During cardiac IR, diminished blood flow leads to insufficient O_2 delivery to mitochondria, resulting in loss of ATP production.[22] Therefore, to understand the underlying mechanisms for potential differential susceptibility to IR injury in the irradiated versus nonirradiated rats, we simultaneously monitored mitochondrial redox state, i.e., reduced nicotinamide adenine dinucleotide (NADH), oxidized flavin adenine dinucleotide (FAD), and cardiac functions in the *ex vivo* perfused rat heart. Mitochondria being the main source of ATP production in cardiomyocytes represent the bulk source of reducing equivalents, NADH and $FADH_2$. The NADH and $FADH_2$ are the primary electron carriers for oxidative phosphorylation (OXPHOS).[24,25] Mitochondrial ATP production is therefore linked to the reducing equivalents supplied by the tricarboxylic acid (TCA) cycle and the intactness of the electron transport chain (ETC), which couples the electron transfer from NADH and $FADH_2$ to OXPHOS. ATP production is a prerequisite for normal cardiac contractility and for maintaining cardiomyocyte ionic homeostasis for cellular viability. Any compromise in this metabolic process contributes to cell death and impaired cardiac function.

In this study, changes in mitochondrial metabolic status during ischemia alone and IR were investigated by optical techniques, fluorometry, and cryoimaging.[26] This is because some of the relevant fluorophores in biological tissue are involved in cellular metabolism and can provide information about the status of cellular bioenergetics.[27] Through optical methods, the NADH and FAD autofluorescence signals can be measured without using exogenous probes. The ratio NADH/FAD, the redox ratio (RR), represents a quantitative metabolic index/biomarker of cardiac function in normal and disease states.[24,28,29] In addition, the use of online fluorometry to assess dynamic changes in the redox state following WTI and during ischemia and IR is important, because it provides a unique opportunity to correlate changes in cardiac function to the transient changes in mitochondrial function.[28] The use of 3-D cryoimaging is to determine whether there are significant differences in the volumetric histograms of the RR following WTI before, during ischemia, and after ischemia (IR), and whether the differences correlate with cardiac function or dysfunction. We postulate that WTI leads to diminished cardiac function, because of oxidation of mitochondrial redox state and this concomitantly would lead to greater susceptibility to ischemia and IR injury.

2 Materials and Methods

The study consisted of six groups of hearts: time controls (TCs) of nonirradiated and irradiated hearts (TCnon and TCirr, respectively), ischemia alone of nonirradiated and irradiated hearts (ISCnon and ISCirr, respectively), and ischemia followed by reperfusion of both nonirradiated (IRnon) and irradiated hearts (IRirr). The TC hearts were perfused for the duration of the IR protocol without ischemia.

2.1 *Whole Thoracic Irradiation*

Unanesthetized female WAG/RijCmcr (Wistar) rats were irradiated in batches, with a single dose of 15 Gy to the whole thorax only as already described.[16] The rats were 9 to 10 weeks of age and weighed 120 to 140 g at the time of irradiation. The irradiated rats were housed with age-matched nonirradiated siblings, which were used as controls. The rats were used for the experimentation at 35 days after irradiation. This time point was chosen for studying the irradiated rats because all rats developed lethal radiation pneumonitis after 45 days.[16]

All experiments conformed to the Guide for the Care and Use of Laboratory Animals and were approved by the Medical College of Wisconsin Institutional Animal Care and Use Committee.

2.2 *Experimental Protocol*

At day 35 after irradiation, the animals were sacrificed, and the hearts were extracted for *ex-vivo* Langendorff perfusion. A combination of ketamine and heparin was given to the animal for sedation and to prevent clotting, respectively. After full anesthesia was verified, rats were decapitated, and their hearts were quickly cannulated and perfused with a cold rat physiological saline. Hearts were transferred to the Langendorff apparatus and perfused at constant pressure of 70 mmHg with the same rat physiological salt solution buffer, which contains (in mM) NaCl 119, KCl 4.7, $MgSO_4$ 1.2 $CaCl_2$ 1.6, $NaHCO_3$ 27.8, EGTA 0.3, NaH_2PO_4 1.2, glucose 5.3, and pyruvate 1.9.[30,31] The buffer was oxygenated with 97% O_2 and 3% CO_2 and kept warm at 37°C.

We have reported extensively on our cardiac IR protocol in previous studies,[26,32–34] which will be adopted in this study of irradiated and nonirradiated rat hearts. In brief, after cannulating the hearts for retrograde perfusion via the aorta, they were left to stabilize for 25 to 30 mins before initiating the ischemia, IR, or TC perfusion protocol. For the ischemia only group, the hearts were subjected to no flow global ischemia for 25 min by constricting the retrograde flow through the aortic cannula. The IR groups underwent similar ischemia for 25 min followed by reperfusion, i.e., removing the aortic constriction, for 60 min. During the whole experimental period, including the ischemic period, the hearts were kept in a circulating water bath at 37°C. The TC hearts were perfused for the same protocol duration as the IR experiments, without ischemia. The TCs are expected to show no significant difference in redox signal intensity and cardiac function over the entire protocol; thus, validating the reliability of the *ex vivo* model for evaluating IR-induced damage.

At the end of each experiment, the hearts were immediately flash frozen in liquid N_2 to preserve the mitochondrial metabolic state, as described in our previous studies.[26,35] To minimize cracks and deformations/damage to the frozen tissue, the hearts were first immersed in chilled liquid isopentane for a couple of minutes before transferring them to liquid N_2. All hearts were stored in −80°C freezer until optical cryoimaging was performed.

2.3 *Measurement of Cardiac Function*

After stabilization, functional parameters were measured online and continuously in the *ex vivo* heart; these included heart rate (HR), systolic left ventricular pressure (LVP) and diastolic pressure (diaLVP), and coronary flow (CF). A saline-filled

balloon connected to a catheter was placed in the left ventricle through an opening in the left atrium, with the catheter distally attached to a pressure transducer to measure LVP isovolumetrically.[33,36,37] The diaLVP was intentionally set at 0 mmHg to monitor diastolic contracture, i.e., an increase in diaLVP during the experiment, reflects left ventricular contracture, an index of cardiac dysfunction. All functional measurements were initiated within 20 min after baseline followed by either ischemia alone, IR, or continuous perfusion (TC) for the duration of the IR protocol. Developed LVP (dLVP) was calculated as the differences between the systolic (maximum; LVP) and the diastolic (minimum; diaLVP) pressures. Spontaneous HR was monitored with bipolar electrodes placed in the right atrial and ventricular walls.[38,39] An ultrasonic flowmeter (Transonic T106X; Ithaca, New York) was placed directly in the aortic inflow line to measure CF. Samples of the buffer and coronary effluent were collected prior to ischemia and during reperfusion to monitor pH changes and ionic compositions during the experiments (data not shown).

The rate pressure product (RPP) was used to estimate cardiac work and calculated as the product of dLVP and HR (RPP = dLVP × HR). To determine the recovery rate of dLVP, the slope of the dLVP signal during the recovery phase of reperfusion was calculated using Eq. (1):

$$\text{Recovery rate} = \frac{\text{dLVP(reperfusion)} - \text{dLVP(ischemia)}}{\Delta t}, \tag{1}$$

where dLVP (reperfusion) and dLVP (ischemia) are the average dLVP during late reperfusion (min 60 to 90) and late ischemia (min 20 to 30), respectively. Δt is the recovery time, which is the time it would take dLVP to reach to its dLVP (reperfusion) peak state.

2.4 *Optical Fluorometry of Mitochondrial Redox State in Intact Beating Hearts Ex Vivo*

Dynamic fluorometric measurements of mitochondrial redox state were assessed using a trifurcated fiber optic probe gently placed against the left ventricular free wall of the beating heart, without impeding cardiac function, as described in our previous studies.[40,41] The fluorometer uses a xenon arc lamp at 85 W for excitation, filtered at 350 nm for NADH, and 480 nm for FAD. The arc lamp shutter opens only for 2.5-s recording intervals to prevent photobleaching. Emission signals were assessed at the ratio of 450 nm/390 nm for NADH and 540 nm for FAD.[24,26,31,34,42] The intensities were measured by photomultipliers (photomultiplier detection system 814, PTI), which were digitized, recorded, and visualized, as previously described.[26] All experiments were performed in a light-proofed Faraday cage to minimize ambient photobleaching. The captured fluorescent signals were normalized by dividing each signal to its own average baseline (min 1 to 5 of experiment).

2.5 *3-D Optical Cryoimaging of Mitochondrial Redox State in Frozen Hearts*

By using our cryoimager to measure autofluorescence signals of NADH and FAD, the RR can be calculated as a three-dimensional (3-D) image at a set freezing time.[24,35] The fluorometer, discussed above, has the advantage that it measures the redox state of a patch of tissue on the LV online either *ex vivo* or *in vivo*; the 3-D cryoimaging has the advantage of measuring fluorescent signal in the whole 3-D organ at freezing time, thereby minimizing effects from sampling error due to heterogeneity across the tissue.

The cryopreserved hearts were imaged in our custom-made cryoimager at the Biophotonics Lab, University of Wisconsin-Milwaukee. To keep the tissue in place for imaging, the frozen hearts were first embedded in a customized black mounting medium for slicing and imaging. The system consists of a freezer set at a cryogenic temperature with an automated acquisition system, which sequentially slices the tissue with a microtome blade and acquires images of up to five fluorophores. The system is illustrated in Fig. 1. A mercury arc lamp (200 W lamp, Oriel, Irvine, California, with light source from Ushio Inc., Japan) is used as a light source, and the light is filtered by selected wavelengths to excite specific fluorophores from the surface of the tissue. The excitation filter for NADH was set at 350 nm (80-nm bandwidth, UV Pass Blacklite, HD Dichroic, Los Angeles, California), and the corresponding FAD filter was set at 437 nm (20-nm bandwidth, 440QV21, Omega Optical, Brattleboro, Vermont). After exciting the fluorophores in the tissue, they emit different wavelengths back, which are filtered by another set of filters and recorded by a camera. Emission filters were set at 460 nm (50-nm bandwidth, D460/50M, Chroma, Bellows Falls, Vermont) and 537 nm (50-nm bandwidth, QMAX EM 510-560, Omega Optical) for NADH and FAD, respectively. All filters were controlled by two motorized filter wheels (Oriental Motor Vexta Step Motor PK268-01B). The images were captured using a charge-coupled camera (QImaging, Rolera EM-C2, 14 bit) with a 1004 × 1002 pixel arrays. The z resolution was 30 μm defined by slicing size. Freezing, embedding, and imaging procedures were conducted as previously described.[24,26]

NADH and FAD autofluorescence images from heart slices were analyzed using MATLAB. As previously described,[24,26] calibration was performed to minimize day-to-day variations in light intensity, mirror angle, and nonuniformity of the illuminations pattern. 3-D rendering of the RR for all hearts were calculated voxel-by-voxel according to Eq. (2):

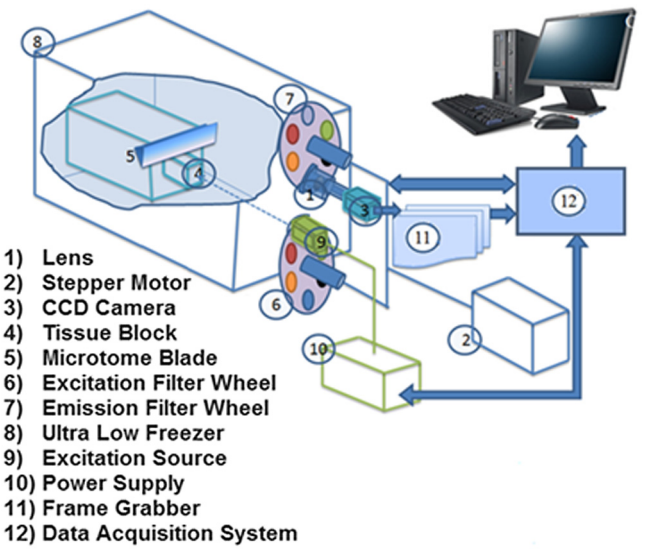

Fig. 1 Schematic illustration of cryoimaging system used in this study. All components are labeled and explained.

$$\mathrm{RR} = \mathrm{NADH}/\mathrm{FAD}, \tag{2}$$

where NADH and FAD are the intensities of NADH voxel and FAD voxel, respectively. Subsequently, the histograms of the RR for each heart, which is a distribution of intensities through the whole volume, were found. The corresponding mean value of each histogram was calculated according to Eq. (3):

$$\mathrm{RR\ mean} = \sum_{i=1}^{N} \mathrm{Heart\_Volume}(i), \tag{3}$$

where N is the total number of voxels within the heart. The mean values of the histograms can be used for quantitative analyses of metabolic states of hearts.

2.6 *Statistical Analysis*

Statistical analysis on cryoimages and fluorometer data was performed using a one-way ANOVA followed by Tukey's posthoc analysis. For fluorometer data, the end time point of each experiment (TC: 90 min, ISC: 25 min, and IR: 90 min) was chosen to do the statistical analysis because it will allow us to compare with the cryo results. Statistical analysis on functional data (CF, dLVP, diaLVP, and RPP) was performed using repeated ANOVA followed by Tukey–Kramer posthoc analysis for multiple comparisons between groups. In all cases, a $p < 0.05$ was used to determine significant differences.

3 Results

Data for the mean value ± standard error of the mean (SEM) of the normalized NADH and FAD fluorescence signals for all the treatment groups (TC, ISC, or IR) are shown in Figs. 2(a) and 2(b), respectively. Figure 2(c) shows the calculated RR using Eq. (2). All measurements were normalized to their own baseline values to eliminate day-to-day, light intensity, and other potential variations. In the nonirradiated and irradiated hearts, the TCs show no change in NADH, FAD, and RR signals during the perfusion protocol. These observations indicate that the redox potential of mitochondria remained stable during the perfusion, and any changes would be attributed to additional stress (e.g., IR) applied to the hearts. When the hearts were exposed to ischemia, in both irradiated and nonirradiated hearts, it caused a significant increase in the RR (54% and 50% increase, respectively) compared to their respective TCs. During reperfusion, the RR decreased by ~14% to 15% for both hearts when compared to their respective TCs or baselines. The differences between IRnon and IRirr for both NADH and FAD during the reperfusion phase were not significant. This indicates that both irradiated and nonirradiated hearts were equally reduced and oxidized during IR stress. These dynamic fluorometric data are consistent with our previous observations.[26]

Figure 3 shows measured functional parameters of CF [Fig. 3(a)], dLVP [Fig. 3(b)], diaLVP [Fig. 3(c)], and calculated RPP [Fig. 3(d)] over time for all treatment groups. Table 1 shows the summary of functional data that compares TC and IR groups with or without irradiation treatments at selected time points during the experiments, with 31 to 35 min and 50 to 90 min corresponding to the early and late reperfusion phases, respectively. In the TCs, all functional parameters remained relatively constant throughout the perfusion protocol (see Fig. 3). These observations also justify the stability and reliability of the *ex vivo* perfused heart model during IR. The TC of the irradiated hearts showed significantly lower basal levels of CF, dLVP, and the RPP compared to the TC of nonirradiated hearts (see Fig. 3 and Table 1). These different responses suggest differences in myocardial work performed by the beating hearts, possibly due to the exposure to radiation. When compared to their respective TCs on reperfusion, CF in the nonirradiated hearts recovered less than the irradiated hearts, resulting in a significant difference between IRnon and TCnon, but no difference for IRirr and TCirr later on reperfusion (see Table 1). These observations imply that the CF of IRirr group was better preserved after ischemia compared to the nonirradiated hearts; the irradiated hearts also recovered from IR injury toward their TCirr basal level [see Fig. 3(a)]. The average of dLVP recovery rate for IRnon and IRirr groups was 25.4 and 1.5 (mmHg/min), respectively, which were significantly different. This result suggests that the IRirr showed a significant delay in recovery of dLVP when compared to the IRnon. However, as reperfusion time progressed, dLVP was not significantly different between the two groups [see Fig. 3(b) and Table 1]. Figure 3(c) shows diastolic LVP (diaLVP), a marker for myocardial contracture or diastolic tone, which impairs cardiac work. diaLVP increased significantly during ischemia and remained significantly elevated on reperfusion in both irradiated and nonirradiated hearts when compared to their respective TCs. Similar diastolic contracture suggests that both irradiated and nonirradiated hearts displayed comparable susceptibility to IR-induced myocardial damage. Figure 3(d) shows the calculated RPP, an index of cardiac work, and it reflects the impact of stress on cardiac muscles. Like dLVP, both irradiated and nonirradiated hearts showed similar magnitude of compromise in RPP. Indeed, and paradoxically, the magnitude of depression of contractile force following IR seems to be more pronounced in the

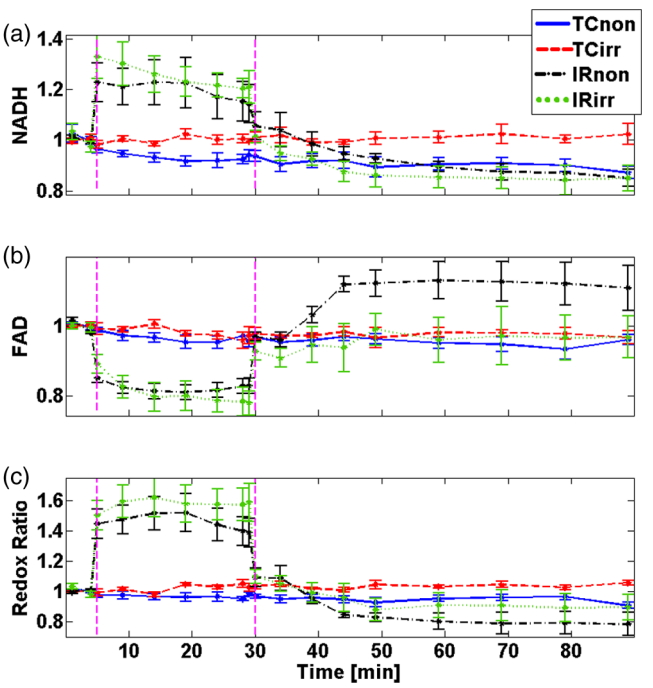

Fig. 2 Mean value ± SEM of fluorometry data of (a) NADH, (b) FAD, and (c) RR signals over time for $n = 4$ to 8/group. Each dataset is normalized to its baseline measurement before calculating the mean for each group. The vertical dashed lines mark time points for start of ischemia or reperfusion.

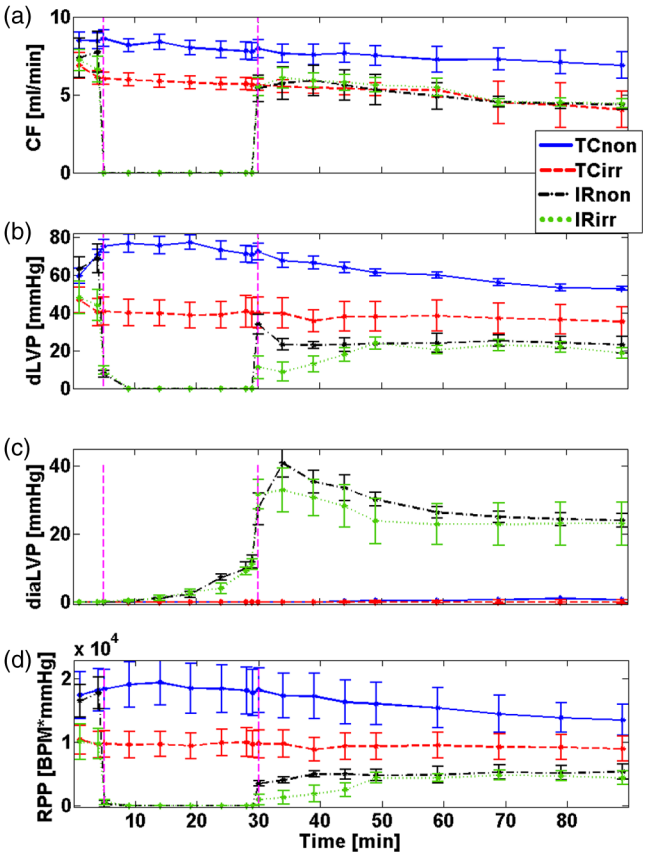

Fig. 3 Changes in CF, dLVP, and diaLVP measured over time in parallel with fluorometry, as well as the calculated RPP. Values are mean values ± SEM for TC and IR hearts for both nonirradiated and irradiated groups ($n = 3$ to 6/group). The vertical dashed lines mark time points for start of ischemia or reperfusion.

nonirradiated hearts compared to the irradiated hearts, with respect to their TCs (see Fig. 3). This portends that irradiation does not predispose the hearts to less cardiac work on reperfusion when compared to the nonirradiated hearts. It is worth noting that HR was not significantly different between the irradiated and nonirradiated hearts (data not shown).

Overall, these results indicate that WTI compromised contractile function and cardiac work. However, low dose WTI before manifestation of pulmonary dysfunction did not lead to a significant increase in susceptibility of the heart to IR injury; cardiac mitochondrial redox state was not significantly altered by the exposure to radiation.

Figure 4(a) shows representative 3-D cryoimages obtained from the different treatment groups (TCnon, TCirr, ISCnon ISCirr, IRnon, IRirr). Representative 3-D rendered RRs from each group are also shown. A difference in the 3-D rendered images can be observed in the different experimental conditions (TC, ISC, and IR); there was no significant difference in the RR between nonirradiated and irradiated hearts under similar experimental conditions. This observation is consistent with the dynamic fluorometric data (Fig. 2); the RRs increased during ischemia and decreased during reperfusion when compared to their respective TCs. The individual representative images for the RR distributions are summarized in the histograms in Fig. 4(b). The weighted mean value calculated using Eq. (3) is shown in the plot legend. As explained in our previous study,[26] a high mean value of RR suggests a reduced redox state of mitochondria, and a low value suggests an oxidized redox state of mitochondria.

Figure 5 shows a summary bar plot of the mean ± SEM of cryoimaging RR for each treatment group. There was a significant difference in RR ($p < 0.05$) between TC and ISC or IR for the irradiated and nonirradiated hearts when compared to their TCs. For nonirradiated and irradiated hearts, ischemia increased RR 78% and 105%, respectively, whereas IR decreased RR by 42% and 55%, respectively. Thus, there was no significant difference in the RR between the two groups, which is consistent with data shown in Fig. 2.

4 Discussion

This study investigated whether irradiated rat hearts, following single dose of 15 Gy WTI, are more susceptible to ischemia and IR injury compared to nonirradiated rat hearts. The study also investigated the role of mitochondrial metabolism (redox state) in the differential susceptibility to IR injury. To the best of our knowledge, this study is the first to investigate the impact of thoracic irradiation on IR injury and the role of mitochondrial metabolic redox state on the cardiac dysfunction that ensue.

Mitochondria are key factors of myocardial tissue energy and redox homeostasis; therefore, compromise in the mitochondrial function leads to cardiomyocytes and endothelial cell death and

Table 1 Mean difference ± SEM of between groups' comparisons for CF, dLVP, diaLVP, and RPP to evaluate the overall performance (min 1 to 90) by TC comparisons and recovery of hearts during early reperfusion phase (min 31 to 35) and final reperfusion injury phase (min 50 to 90).

		CF (ml/min)	dLVP (mmHg)	diaLVP (mmHg)	RPP (HR × mmHg)
TCirr versus Tcnon	min 1 to 90	−2.23 ± 0.67[a]	−29.12 ± 4.88[a]	−0.11 ± 3.57	−7835 ± 2971[a]
IRirr versus IRnon	min 31 to 35	0.13 ± 0.89	−15.93 ± 5.26[a]	−7.84 ± 6.79	−2030 ± 2501
	min 50 to 90	0.20 ± 0.73	−2.50 ± 4.63	−5.55 ± 5.78	−1381 ± 2386
IRnon versus TCnon	min 31 to 35	−2.01 ± 0.94	−43.42 ± 5.94[a]	37.40 ± 7.12[a]	−14,431 ± 2623[a]
	min 50 to 90	−2.49 ± 0.76[a]	−32.60 ± 4.85[a]	25.37 ± 6.06[a]	−10,840 ± 2502[a]
IRirr versus TCirr	min 31to 35	0.27 ± 1.09	−30.07 ± 6.94[a]	29.56 ± 8.31[a]	−8769 ± 3064[a]
	min 50 to 90	0.21 ± 0.89	−15.50 ± 5.67	20.42 ± 7.08[a]	−5646 ± 2922

[a]Indicates significant difference.

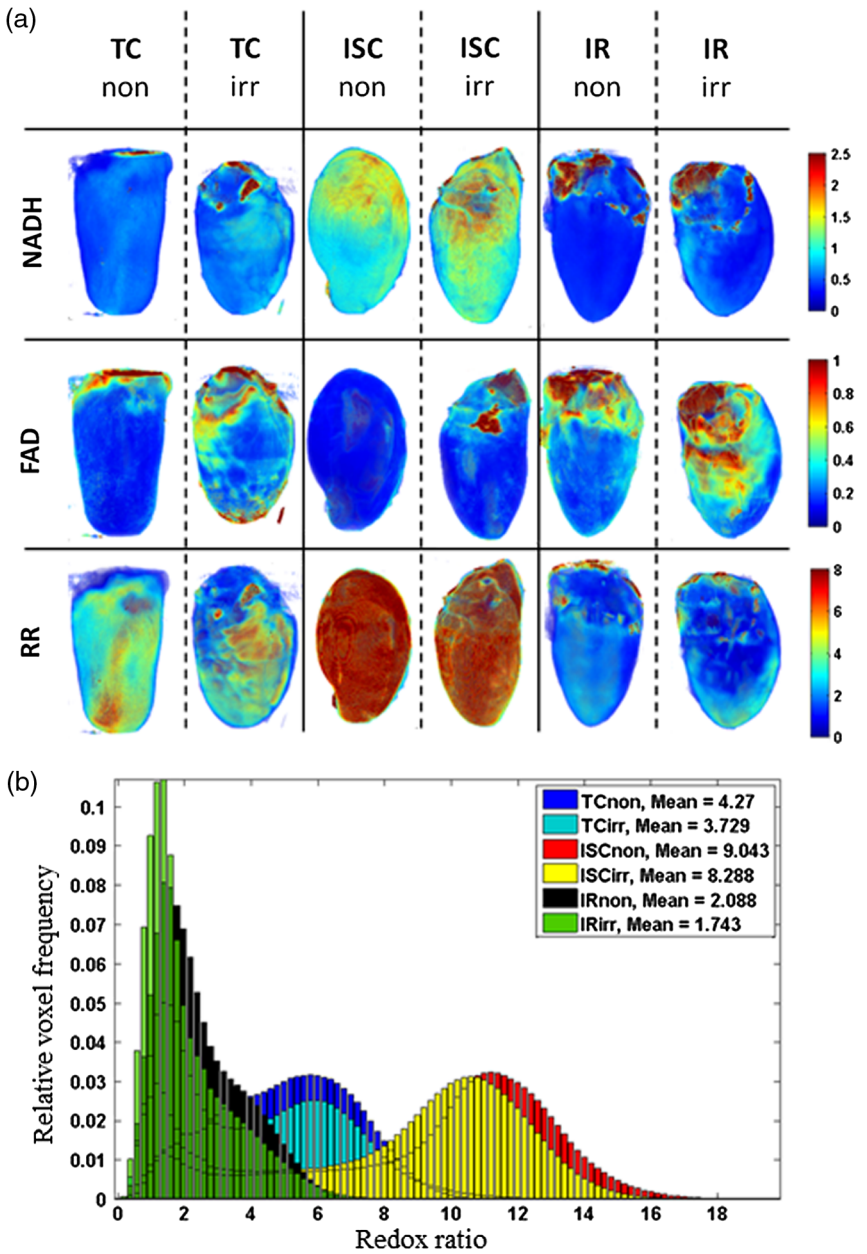

Fig. 4 Cryoimaging results of representative hearts in each group. (a) 3-D fluorescent images of NADH, FAD, and RR. (b) Corresponding histograms of voxel distribution of the RR fluorescent images.

hence, cardiovascular abnormalities. Since mitochondria are responsible for the bulk ATP produced in the heart, any perturbations in the biochemical machinery of OXPHOS are expected to impair ATP generation. Mitochondrial ATP production is linked to the reducing equivalents, $NADH/FADH_2$, supplied by the TCA cycle, the intactness of the ETC to couple electron transfer from the reducing equivalents to ATP production, which is necessary for contractility and maintaining ionic homeostasis in cardiomyocytes. Altered mitochondrial function on reperfusion will lead to dysfunction in ATP production and concomitantly, poor contractile function, i.e., decrease dLVP and increase diaLVP (Fig. 3 and Table 1).

Insofar as mitochondria are the powerhouse of cardiomyocytes, they are the major contributors of the redox state, with negligible contributions from cytoplasmic sources.[43–45] In the current study, we used 3-D optical cryoimaging and dynamic fluorometry to measure mitochondrial redox state (NADH, FAD, and NADH/FAD or RR) as an index of bioenergetics before, during, and after global ischemia and IR. Our results show that there is no significant difference in the redox state before ischemia, and the changes in redox state during ischemia and IR for both irradiated and nonirradiated hearts are similar and consistent with our previous results.[26,31,32,34,40] That is, ischemia caused a marked reduction of the redox state, while reperfusion caused oxidation of the mitochondrial redox state for both nonirradiated and irradiated hearts. The increase in RR in the hearts during ischemia is due to lack of O_2 supplies to the myocardium, with concomitant decrease in electron transfer from NADH and $FADH_2$. The oxidation of the mitochondrial redox state on reperfusion tended to be more pronounced in the irradiated hearts, albeit not significant (Fig. 4). This observation suggests that mitochondrial metabolism was

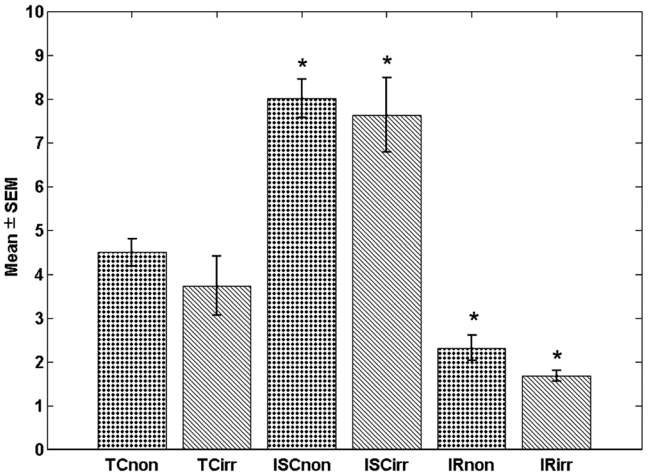

Fig. 5 Bar plot of mean ± SEM for volumetric histograms showing statistical analysis ($n = 5$/group). * shows the group that are significantly different from their respective TCs. Significant difference is observed between different treatments, but not intergroup, i.e., nonirradiated versus irradiated samples with same treatment.

not altered after WTI. Furthermore, the similarities in redox state in the two groups before, during, and after ischemia suggest that cardiomyocyte mitochondrial physiology was preserved during exposure to the brief pulse of WTI.

Increase in the oxidized state of mitochondria following ischemia could be ascribed to, in part, impaired ETC function and OXPHOS. A higher NADH oxidation without concomitant increase in ATP production suggests an increase reactive oxygen/nitrogen species (ROS/RNS) production, which are contributing factors in IR injury.[36,37,46] We showed previously that ROS and RNS production increase dynamically in the *ex vivo* perfused heart during ischemia and on reperfusion, and the magnitude of cardiac functional recovery correlated with the extent of ROS or RNS produced. Thus, cardioprotective interventions that mitigate IR damage and improve functional recovery on reperfusion show significant attenuation of ROS emission during ischemia and on reperfusion.[42] Our functional data in the current study infer that WTI may not predispose irradiated hearts to more ROS production during IR and hence, worsening of cardiac function.

The compromise in cardiac function (dLVP, CF, and RPP) under basal conditions (TCs) in the irradiated hearts could be due to radiation-induced damage to cardiac tissue, independent of impact on mitochondrial bioenergetics. Consistent with our observations, other studies have shown that irradiation induces cardiac dysfunction.[2,12–14] Although we did not measure ROS in the current study, others have reported that radiation treatment causes direct damage to blood vessels by generating ROS.[47] It is worth noting that even though dLVP and CF were lower in the irradiated hearts under basal conditions, i.e., TC, they remained relatively constant throughout the perfusion period. In fact, the CF and dLVP decreased with time in the nonirradiated TC-perfused hearts to the steady levels of the irradiated hearts, indicating that "cardiac reserve" may be compromised by radiation. During the initial reperfusion period, dLVP of the irradiated hearts also recovered slower than the nonirradiated hearts; at the end of reperfusion, dLVP and CF in the irradiated hearts recovered to the same level as their TCs or basal levels, while in the nonirradiated hearts, dLVP and CF were significantly lower compared to their TCs or basal levels. The constancy of CF in the TC irradiated hearts and the near-full return to basal level on reperfusion suggests that the effect of irradiation on the vasculature had reached a maximal effect, and additional stressor would not affect flow. This notion is consistent with our observation in pulmonary vessels rings, *ex vivo*, obtained from irradiated rats, which displayed less change to vasoactive agents compared to vessel rings from nonirradiated pulmonary vessels.[48]

High single dose of irradiation ≥18 Gy or fractionated doses of ≥36 Gy have been reported to cause acute pericarditis within 3 to 6 months[17,20,49] after initial exposure. At lower doses, signs of damage are primarily manifested in microvessels.[15,19,49] The method of administering the thoracic irradiation also seems to differentially impact cardiac function. For example, it was shown that irradiating whole lungs resulted in greater damage to the heart than irradiating four small thoracic regions with similar dose.[50,51] Considering these previous works, it shows that lower doses and large volumes of exposure to irradiation used in our experiments would exert considerable effects on heart and lung functions. Indeed, most of these animals succumb to the irradiation damage beyond 35 days due to complications in both cardiac and pulmonary function.[16] Interestingly, our current study shows that despite the injurious effects of the WTI on the cardiovascular system, it does not predispose the hearts to further damage following ischemic incident. This observation may have clinical implications, because of the common use of radiotherapy.

In conclusion, local irradiation to the thoracic region is commonly used for cancer treatment and medical imaging. The mechanisms of cardiac IR injury and the effects of irradiation on the heart have been investigated in animal models; however, to our knowledge, no study has looked at the potential for increased susceptibility to IR injury and the role of mitochondrial metabolism following WTI. We did not observe any significant difference in the redox state of mitochondria between the irradiated and nonirradiated hearts, and irradiation did not lead to aggravated reperfusion injury. Overall, the functional data show that even though the WTI hearts showed some compromise in their basal function, they performed equally as well as the nonirradiated hearts during ischemia and IR; mitochondria metabolic state was not different between the two groups.

Disclosures

The authors declare that there are no conflicts of interest related to this article.

Acknowledgments

We acknowledge the Radiation Biology Service Center at the Medical College of Wisconsin (MCW) for irradiation and dosimetry services. We thank Brian Fish, Jayashree Narayanan, Tracy Gasperetti, and Marylou Mader for excellent technical support and Alexis Visotcky for statistical advice. M. R. funded by UWM RGI 101X290, and M. M. funded by NIAID R01-101898, U01-107305, Department of Radiation Oncology, MCW and NIH grant R01HL116530.

References

1. National Center for Health Statistics, "Health, United States, 2016: with chartbook on long-term trends in health," Hyattsville, Maryland (2017).
2. C. G. Lenneman and D. B. Sawyer, "Cardio-oncology an update on cardiotoxicity of cancer-related treatment," *Circ. Res.* **118**(6), 1008–1020 (2016).

3. E. Senkus-Konefka and J. Jassem, "Cardiovascular effects of breast cancer radiotherapy," *Cancer Treat. Rev.* **33**(6), 578–593 (2007).
4. G. Gagliardi et al., "Long-term cardiac mortality after radiotherapy of breast cancer—application of the relative seriality model," *Br. J. Radiol.* **69**(825), 839–846 (1996).
5. G. Pili et al., "Geometric and dosimetric approach to determine probability of late cardiac mortality in left tangential breast irradiation: comparison between wedged beams and field-in-field technique," *Int. J. Radiat. Oncol. Biol. Phys.* **81**(3), 894–900 (2011).
6. B. Seddon et al., "Detection of defects in myocardial perfusion imaging in patients with early breast cancer treated with radiotherapy," *Radiother. Oncol.* **64**(1), 53–63 (2002).
7. D. L. Preston et al., "Studies of mortality of atomic bomb survivors. Report 13: solid cancer and noncancer disease mortality: 1950–1997," *Radiat. Res.* **160**(4), 381–407 (2003).
8. M. Yamada et al., "Noncancer disease incidence in atomic bomb survivors, 1958–1998," *Radiat. Res.* **161**(6), 622–632 (2004).
9. J. E. Baker, J. E. Moulder, and J. W. Hopewell, "Radiation as a risk factor for cardiovascular disease," *Antioxid. Redox Signaling* **15**(7), 1945–1956 (2011).
10. B. J. Geist et al., "Physiologic consequences of local heart irradiation in rats," *Int. J. Radiat. Oncol. Biol. Phys.* **18**(5), 1107–1113 (1990).
11. E. J. Hall and A. J. Giaccia, *Radiobiology for the Radiologist*, Wolters Kluwer Health/Lippincott Williams and Wilkins, Philadelphia (2012).
12. F. Stewart, S. Hoving, and N. Russell, "Vascular damage as an underlying mechanism of cardiac and cerebral toxicity in irradiated cancer patients," *Radiat. Res.* **174**(6b), 865–869 (2010).
13. M. Boerma and M. Hauer-Jensen, "Preclinical research into basic mechanisms of radiation-induced heart disease," *Cardiol. Res. Pract.* **2011**, 858262 (2010).
14. A. Sardaro et al., "Radiation-induced cardiac damage in early left breast cancer patients: risk factors, biological mechanisms, radiobiology, and dosimetric constraints," *Radiother. Oncol.* **103**(2), 133–142 (2012).
15. M. J. Adams et al., "Radiation-associated cardiovascular disease," *Crit. Rev. Oncol./Hematol.* **45**(1), 55–75 (2003).
16. M. Medhora et al., "Whole-thorax irradiation induces hypoxic respiratory failure, pleural effusions and cardiac remodeling," *J. Radiat. Res.* **56**(2), 248–260 (2015).
17. L. Fajardo and J. Stewart, "Experimental radiation-induced heart disease. I. Light microscopic studies," *Am. J. Pathol.* **59**(2), 299–316 (1970).
18. J. E. Baker et al., "10 Gy total body irradiation increases risk of coronary sclerosis, degeneration of heart structure and function in a rat model," *Int. J. Radiat. Biol.* **85**(12), 1089–1100 (2009).
19. S. Schultz-Hector and K.-R. Trott, "Radiation-induced cardiovascular diseases: is the epidemiologic evidence compatible with the radiobiologic data?" *Int. J. Radiat. Oncol. Biol. Phys.* **67**(1), 10–18 (2007).
20. S. Lauk et al., "Radiation-induced heart disease in rats," *Int. J. Radiat. Oncol. Biol. Phys.* **11**(4), 801–808 (1985)
21. T. Yeung and J. Hopewell, "Effects of single doses of radiation on cardiac function in the rat," *Radiother. Oncol.* **3**(4), 339–345 (1985).
22. L. M. Buja, "Myocardial ischemia and reperfusion injury," *Cardiovasc. Pathol.* **14**(4), 170–175 (2005)
23. A. Frank et al., "Myocardial ischemia reperfusion injury from basic science to clinical bedside," *Semin. Cardiothorac. Vasc. Anesth.* **16**, 123–132 (2012).
24. R. Sepehr et al., "Optical imaging of tissue mitochondrial redox state in intact rat lungs in two models of pulmonary oxidative stress," *J. Biomed. Opt.* **17**(4), 046010 (2012).
25. H. N. Xu and L. Z. Li, "Quantitative redox imaging biomarkers for studying tissue metabolic state and its heterogeneity," *J. Innovative Opt. Health Sci.* **7**(2), 1430002 (2014).
26. M. Ranji et al., "Optical cryoimaging reveals a heterogeneous distribution of mitochondrial redox state in ex vivo guinea pig hearts and its alteration during ischemia and reperfusion," *IEEE J. Transl. Eng. Health Med.* **4**, 1800210 (2016).
27. V.-D. Tuan, *Biomedical Photonics Handbook*, CRC Press Inc., Boca Raton, Florida (2003).
28. M. Ranji et al., "Quantifying acute myocardial injury using ratiometric fluorometry," *IEEE Trans. Biomed. Eng.* **56**(5), 1556–1563 (2009).
29. B. Quistorff, J. C. Haselgrove, and B. Chance, "High spatial resolution readout of 3-D metabolic organ structure: an automated, low-temperature redox ratio-scanning instrument," *Anal. Biochem.* **148**(2), 389–400 (1985).
30. M. Aldakkak et al., "Modulation of mitochondrial bioenergetics in isolated guinea pig beating heart by potassium and lidocaine cardioplegia: implications for cardioprotection," *J. Cardiovasc. Pharmacol.* **54**(4), 298–309 (2009).
31. A. K. Camara et al., "ROS scavenging before 27°C ischemia protects hearts and reduces mitochondrial ROS, Ca^{2+} overload, and changes in redox state," *Am. J. Physiol.-Cell Physiol.* **292**(6), C2021–C2031 (2007).
32. M. L. Riess et al., "Altered NADH and improved function by anesthetic and ischemic preconditioning in guinea pig intact hearts," *Am. J. Physiol.-Heart Circ. Physiol.* **283**(1), H53–H60 (2002).
33. M. L. Riess et al., "Preconditioning with sevoflurane reduces changes in nicotinamide adenine dinucleotide during ischemia-reperfusion in isolated hearts reversal by 5-hydroxydecanoic acid," *J. Am. Soc. Anesthesiol.* **98**(2), 387–395 (2003).
34. J. An et al., "Warm ischemic preconditioning improves mitochondrial redox balance during and after mild hypothermic ischemia in guinea pig isolated hearts," *Am. J. Physiol. Heart Circ. Physiol.* **288**(6), H2620–H2627 (2005).
35. F. Salehpour et al., "Effects of p67phox on the mitochondrial oxidative state in the kidney of Dahl salt-sensitive rats: optical fluorescence 3-D cryoimaging," *Am. J. Physiol.-Renal Physiol.* **309**(4), F377–F382 (2015).
36. A. K. Camara, M. Bienengraeber, and D. F. Stowe, "Mitochondrial approaches to protect against cardiac ischemia and reperfusion injury," *Front. Physiol.* **2**, 13 (2011).
37. D. F. Stowe and A. K. Camara, "Mitochondrial reactive oxygen species production in excitable cells: modulators of mitochondrial and cell function," *Antioxid. Redox Signaling* **11**(6), 1373–1414 (2009).
38. A. K. Camara et al., "Na^+/H^+ exchange inhibition with cardioplegia reduces cytosolic $[Ca^{2+}]$ and myocardial damage after cold ischemia," *J. Cardiovasc. Pharmacol.* **41**(5), 686–698 (2003).
39. Q. Chen et al., "Modulation of electron transport protects cardiac mitochondria and decreases myocardial injury during ischemia and reperfusion," *Am. J. Physiol.-Cell Physiol.* **292**(1), C137–C147 (2007).
40. M. Aldakkak et al., "Ranolazine reduces Ca^{2+} overload and oxidative stress and improves mitochondrial integrity to protect against ischemia reperfusion injury in isolated hearts," *Pharmacol. Res.* **64**(4), 381–392 (2011).
41. M. Aldakkak et al., "Enhanced Na+/H+ exchange during ischemia and reperfusion impairs mitochondrial bioenergetics and myocardial function," *J. Cardiovasc. Pharmacol.* **52**(3), 236–244 (2008)
42. M. Aldakkak et al., "Inhibited mitochondrial respiration by amobarbital during cardiac ischaemia improves redox state and reduces matrix Ca^{2+} overload and ROS release," *Cardiovasc. Res.* **77**(2), 406–415 (2008).
43. L. A. Katz, A. P. Koretsky, and R. S. Balaban, "Respiratory control in the glucose perfused heart: a 31P NMR and NADH fluorescence study," *FEBS Lett.* **221**(2), 270–276 (1987).
44. R. W. Estabrook, "Fluorometric measurement of reduced pyridine nucleotide in cellular and subcellular particles," *Anal. Biochem.* **4**(3), 231–245 (1962).
45. E. Nuutinen, "Subcellular origin of the surface fluorescence of reduced nicotinamide nucleotides in the isolated perfused rat heart," *Basic Res. Cardiol.* **79**(1), 49–58 (1984).
46. A. K. Camara, E. J. Lesnefsky, and D. F. Stowe, "Potential therapeutic benefits of strategies directed to mitochondria," *Antioxid. Redox Signaling* **13**(3), 279–347 (2010).
47. O. A. Hatoum et al., "Radiation induces endothelial dysfunction in murine intestinal arterioles via enhanced production of reactive oxygen species," *Arterioscler. Thromb. Vasc. Biol.* **26**(2), 287–294 (2006).
48. R. Zhang et al., "Structural and functional alterations in the rat lung following whole thoracic irradiation with moderate doses: injury and recovery," *Int. J. Radiat. Biol.* **84**(6), 487–497 (2008).
49. F. Stewart, "Mechanisms and dose-response relationships for radiation-induced cardiovascular disease," *Ann. ICRP* **41**(3), 72–79 (2012).
50. V. A. Semenenko et al., "Irradiation of varying volumes of rat lung to same mean lung dose: a little to a lot or a lot to a little?" *Int. J. Radiat. Oncol. Biol. Phys.* **71**(3), 838–847 (2008).
51. G. Ghobadi et al., "Physiological interaction of heart and lung in thoracic irradiation," *Int. J. Radiat. Oncol. Biol. Phys.* **84**(5), e639–e646 (2012).

Mette Funding la Cour received her BSc and MSc degrees in microtechnology from Technical University of Denmark (DTU). She finished her PhD at the Center for Fast Ultrasound Imaging and MEMS-Applied Sensors at DTU in 2014 with research focus on microfabrication of capacitive micromachined ultrasonic transducers for medical imaging. She worked from 2015 to 2017 in Biophotonics Lab, University of Wisconsin, Milwaukee, with research in 3-D optical cryoimaging of metabolic markers in biological samples. Currently, she is employed at TTP as a microfabrication specialist.

Shima Mehrvar received her master's degree in biomedical engineering from Amirkabir University of Technology, Tehran, Iran, in 2013. She is currently a PhD student in electrical engineering, University of Wisconsin Milwaukee, United States. Her research interests include biomedical optics, fluorescence spectroscopy and microscopy, signal and image processing.

James S. Heisner received his BSc degree from UW-Oshkosh. He is currently a research associate and the lab manager of the Stowe/Camara Labortory in the Department of Anesthesiology, Medical College of Wisconsin. He has worked in this laboratory for over 25 years, and he has coauthored numerous articles with members of the lab. His areas of expertise are in small animal surgeries, e.g., isolated *ex vivo* heart perfusion and *in vivo* techniques, and isolated mitochondrial studies.

Mohammad Masoudi Motlagh received his bachelor's degree in controls and instrumentation from Shiraz University, Iran, and his MSc degree from the University of Wisconsin-Milwaukee with a research focus in biophotonics. He is currently a senior electrical engineer with Baxter Healthcare Co, Round Lake, Illinois.

Meetha Medhora is a professor of radiation oncology, pulmonary medicine, and physiology at the Medical College of Wisconsin. Her research goal is to identify mechanisms and agents to mitigate delayed injury to the lungs and other organs after exposure to radiation. She also investigates biomarkers to predict radiation-lung injury using SPECT imaging and circulating microRNA profiles. She has recently investigated cross-talk between the lung and the heart after irradiation.

Mahsa Ranji is an associate professor of electrical engineering at the University of Wisconsin-Milwaukee (UWM). She has received her PhD in electrical engineering from University of Pennsylvania followed by a postdoctoral training at Sanford-Burnham Medical research institute in La Jolla, California. Specializing in biomedical optics, her focus is in developing noninvasive tissue diagnostic tools. She is the director of the UWM Biophotonics Laboratory, which focuses on optical imaging, particularly, fluorescence imaging, bioinstrumentation design, and image processing tool development for biomedical applications. She collaborates with clinicians at the Medical College of Wisconsin to study tissue metabolism in cardiopulmonary diseases using optical imaging.

Amadou K. S. Camara received his PhD in renal and cardiovascular physiology from the Department of Physiology, Medical College of Wisconsin (MCW). He is currently a professor in the Department of Anesthesiology, MCW. His research is focused on cardiac oxidative stress and the role of mitochondria. He has authored over 90 articles in peer-reviewed scientific journals and several book chapters, with a majority of the publications dedicated to mechanisms of mitochondrial dysfunction in cardiac ischemia–reperfusion injury.